Harmful Algae 124 (2023) 102388

Contents lists available at ScienceDirect

Harmful Algae

journal homepage: www.elsevier.com/locate/hal

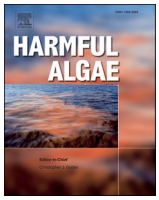

Structure and toxicity of AZA-59, an azaspiracid shellfish poisoning toxin produced by *Azadinium poporum* (Dinophyceae)

Jan Tebben [a,*], Christian Zurhelle [b], Aurelia Tubaro [c], Ingunn A. Samdal [d], Bernd Krock [a], Jane Kilcoyne [e], Silvio Sosa [c], Vera L. Trainer [f], Jonathan R. Deeds [g], Urban Tillmann [a,*]

[a] *Alfred Wegener Institute, Helmholtz Centre for Polar and Marine Research, Section Ecological Chemistry, Am Handelshafen 12, Bremerhaven, 27570, Germany*
[b] *University of Bremen, Department of Biology and Chemistry, Marine Chemistry, Leobener Straße 6, Bremen, 28359, Germany*
[c] *Department of Life Sciences, University of Trieste, Via A. Valerio 6, Trieste, 34127, Italy*
[d] *Norwegian Veterinary Institute, P.O. Box 641431 Ås, Norway*
[e] *Marine Institute, Rinville, Oranmore, County Galway H91 R673, Ireland*
[f] *Olympic Natural Resources Center, University of Washington, 1455 S. Forks Ave, Forks, WA 98331, United States*
[g] *Center for Food Safety and Applied Nutrition, Office of Regulatory Science, U.S. Food and Drug Administration, 5001 Campus Drive, College Park, Maryland, 20740, United States of America*

ARTICLE INFO

Editor: Dr Satoshi Nagai

Keywords:
Azaspiracids
Toxicity equivalency factor
Marine phycotoxins
Azaspiracid shellfish poisoning

ABSTRACT

To date, the putative shellfish toxin azaspiracid 59 (AZA-59) produced by *Azadinium poporum* (Dinophyceae) has been the only AZA found in isolates from the Pacific Northwest coast of the USA (Northeast Pacific Ocean). Anecdotal reports of sporadic diarrhetic shellfish poisoning-like illness, with the absence of DSP toxin or *Vibrio* contamination, led to efforts to look for other potential toxins, such as AZAs, in water and shellfish from the region. *A. poporum* was found in Puget Sound and the outer coast of Washington State, USA, and a novel AZA (putative AZA-59) was detected in low quantities in SPATT resins and shellfish. Here, an *A. poporum* strain from Puget Sound was mass-cultured and AZA-59 was subsequently purified and structurally characterized. In vitro cytotoxicity of AZA-59 towards Jurkat T lymphocytes and acute intraperitoneal toxicity in mice in comparison to AZA-1 allowed the derivation of a provisional toxicity equivalency factor of 0.8 for AZA-59. Quantification of AZA-59 using ELISA and LC-MS/MS yielded reasonable quantitative results when AZA-1 was used as an external reference standard. This study assesses the toxic potency of AZA-59 and will inform guidelines for its potential monitoring in case of increasing toxin levels in edible shellfish.

1. Introduction

Azaspiracids (AZAs) are lipophilic marine phycotoxins that can cause shellfish poisoning in humans. Thus far, all confirmed azaspiracid shellfish poisoning (AZP) events, including the first documented case in 1995, were linked to the consumption of shellfish originating from Irish coastal waters (Satake et al., 1998a, 1998b; Twiner et al., 2008). Since the identification and characterization of the first AZA-producing dinoflagellate *Azadinium spinosum* (Tillmann et al., 2009) AZA producing Amphidomataceae have been found in the Atlantic and Pacific oceans (Tillmann, 2018), suggesting AZA contamination as a globally relevant threat to shellfish aquaculture and human health. Currently, more than 70 AZA analogues (Krock et al., 2019; Krock et al., unpublished data) were found in plankton samples, dinoflagellate cultures of some species of *Azadinium* and *Amphidoma,* or shellfish. The minority of AZAs were confirmed by NMR spectroscopy with the remaining postulated from LC-MS/MS analyses. Only three AZAs (AZA-1, -2, and -3) are currently regulated in Europe under 853/2004/EC with a limit of 160 μg AZA-1 equivalents per kg of shellfish meat. In the United States, the US Food and Drug Administration (US FDA) has also established a guidance value for AZAs in shellfish of 160 μg AZA-1 equivalents kg^{-1} (FDA, 2022).

The toxicity of AZAs in humans is still poorly understood but the symptoms are similar to those of diarrheic shellfish poisoning (DSP) including nausea, vomiting, diarrhea, and stomach cramps. AZP symptoms can last for 2–3 days but there are no documented fatal cases or adverse long-term effects. Due to limited data on AZP in humans, most information on AZA toxicity is derived from in vitro and in vivo

* Corresponding authors.
E-mail addresses: jan.tebben@awi.de (J. Tebben), urban.tillmann@awi.de (U. Tillmann).

https://doi.org/10.1016/j.hal.2023.102388
Received 1 December 2022; Received in revised form 13 January 2023; Accepted 18 January 2023
Available online 22 January 2023

experiments (Hess et al., 2014; Twiner et al., 2008). The initial in vivo toxicity study on partially purified AZA-1, carried out in mice, identified an intraperitoneal (i.p.) lethal dose within the range of 150–200 μg kg^{-1}, with stomach and liver swelling and concurrent size reduction of the lymphoid organs (Satake et al., 1998a, 1998b). Injection (i.p.) of purified AZAs in mice induced progressive paralysis of the limbs, dyspnea, and convulsions before death (Furey et al., 2010; Twiner et al., 2008). Subsequent studies in mice determined the i.p. lethal doses of AZA-2 and AZA-3 at 110 and 140 μg kg^{-1}, respectively, with interim toxicity equivalency factors (TEFs) of 1.0, 1.8, and 1.4 for AZA-1, -2, and -3, respectively (Satake et al., 1998b; Ofuji et al., 1999; EFSA, 2008). A more recent i.p. toxicity study in mice determined the median lethal dose (LD_{50}) for AZA-1, -2, and -3, finding AZA-1 ~2.7 times more potent than originally estimated (LD_{50} = 74 μg kg^{-1} versus its previously determined lethal dose of 200 μg kg^{-1}) while the lethal potency of AZA-2 (LD_{50} = 117 μg kg^{-1} versus its lethal dose of 110 μg kg^{-1}) and AZA-3 (LD_{50} = 164 μg kg^{-1} versus its lethal dose of 140 μg kg^{-1}) were both consistent with earlier studies (Kilcoyne et al., 2014a). Considering AZA-1 as the reference toxin, the following new proposed TEFs were calculated from these i.p. LD_{50} values: 1.0 (AZA-1), 0.6 (AZA-2), and 0.5 (AZA-3) (Kilcoyne et al., 2014a).

The acute lethal potency of orally administered AZA-1, -2, and -3 in mice was lower than in i.p. injection studies, with LD_{50} values of 443 μg kg^{-1}, 626 μg kg^{-1}, and 875 μg kg^{-1}, respectively (Pelin et al., 2018). Nevertheless, the TEFs derived from the oral LD_{50} values (TEF = 1.0, 0.7, and 0.5 for AZA-1, -2, and -3, respectively) were comparable to those recorded by the recent i.p. toxicity study (Kilcoyne et al., 2014a) and were recommended for regulatory purposes as correction factors to determine the total AZAs concentration in shellfish (Pelin et al., 2018). Synthetic AZA analogues and partial structures of AZA-1 have also been evaluated for their acute toxicity in mice (Ito et al., 2006). Interestingly, only AZA-1 and its diastereoisomer C1-C20-*epi*-AZA-1 showed significant adverse effects, suggesting that the entire molecule is required to elicit toxicity (Ito et al., 2006).

The cellular targets of AZAs and their potential mode of action have been investigated in vitro on various cell lines, with the majority of studies focusing on cytotoxicity or cell alterations (Alfonso et al., 2005; Bellocci et al., 2010; Boente-Juncal et al., 2018, 2020, 2021; Ito et al., 2002; Kellmann et al., 2009; Pelin et al., 2019; Roman et al., 2002; Ronzitti et al., 2007; Twiner et al., 2012a–c; Twiner et al., 2005; Vale et al., 2007a,b, 2008, Vilarino et al., 2007, 2008). Similar to the mode of action of other phycotoxins, ion channels were identified as a potential target of AZAs (Boente-Juncal et al., 2020, 2021; Ferreiro et al., 2014; Kulagina et al., 2006).

Sporadic anecdotal reports from consumers that experienced DSP-like symptoms after eating shellfish from Puget Sound (Washington State, Pacific Northwest coast of the USA), with no apparent diarrhetic shellfish toxins or *Vibrio* contamination detected, suggested the potential presence of other toxins, such as AZAs, in the region (Trainer et al., 2013). Following up on these reports, Kim et al. (2017) isolated and cultivated multiple *Azadinium* spp. from sediment samples collected in Puget Sound including *A. poporum* Tillmann & Elbrächter, *A. cuneatum, A. obesum,* and *A. dalianense*. Among these, only strains of *A. poporum* were found to produce AZA-like compounds. LC-MS/MS fragmentation data on cell pellet extracts suggested a novel AZA (AZA-59) produced by these *A. poporum* strains. A follow-up study found *A. poporum* to be widely distributed on the outer coast and throughout the inland waters of Washington State and detected AZA-59 in low quantities in both Solid Phase Adsorption Toxin Tracking (SPATT) resins and shellfish (Adams et al., 2020; unpublished data). To date, AZA-59 has been the only AZA found in isolates from the Puget Sound region. Since its first description in 2017, low levels of AZA-59, along with higher amounts of AZA-40 and AZA-2, have also been detected in *A. poporum* strains isolated from the Eastern Mediterranean Sea (Luo et al., 2018).

In the United States, the sanitary control of bivalve molluscan shellfish produced and sold for domestic consumption is managed under a Federal/State cooperative program known as the National Shellfish Sanitation Program (NSSP). Under the NSSP, chemical methods such as HPLC or LC/MS for the determination of AZAs other than AZA-1 would require the use of TEFs to convert values into AZA-1 equivalent concentrations to match the guidance level of 160 μg AZA-1 eq. per kg shellfish meat.

Due to the presence of low levels of AZA-59 in shellfish-producing regions on the Pacific Northwest coast of the United States, toxicological data and a reliable TEF for this toxin are urgently required to inform regulatory policies. Here, AZA-59 was purified and structurally elucidated from a mass culture of an *A. poporum* strain originally isolated from Puget Sound. The in vitro cytotoxicity of AZA-59 towards Jurkat T lymphocytes was tested in comparison to AZA-1. Furthermore, the acute i.p. toxicity in mice was tested in combination to derive a provisional TEF for AZA-59 in comparison to AZA-1. Finally, the ELISA and LC-MS/MS methods were used to determine relative response factors of AZA-59 in comparison to the AZA-1 reference standard. This study will inform guidelines for the potential monitoring of this toxin in the United States, or elsewhere, in case toxin levels in edible shellfish increase in the future.

2. Materials and methods

2.1. Materials and mass culturing

Azadinium poporum strain 121E10 was originally isolated from incubated sediment samples of Puget Sound, Washington State (USA) (Kim et al., 2017). All reagents were purchased from Sigma-Aldrich (Taufkirchen, Germany) unless stated otherwise. A 200 L culture of strain 121E10 was grown in filtered North Sea water enriched with half-strength K-medium (Keller et al., 1987) slightly modified by replacing the organic phosphorus source by 3.62 μM Na_2HPO_4 and by omitting ammonia and with full strength concentration of vitamins. Cells were separated from the culture fluid by continuous flow centrifugation (WVOdesigns, North Charleston, SC, USA) at 2000 g. The supernatant was directly run through a pre-conditioned styrene-divynilbenzene column (15×310 mm, 250–850 μm particle size, Diaion HP-20) which was desalted with ultrapure water (Millipore-Merck, Darmstadt, Germany) and eluted with methanol. The retained algal cell pellet was freeze dried and extracted with acetone. The acetone extract was diluted with ultrapure water to a final concentration of 7% acetone, loaded onto a HP-20 column (dimensions 40 mm x 150 mm), desalted and eluted with methanol. Dai et al. (2019) predominently found AZA-59 in extracts from cell pellets of Pacific *A. poporum* strains in exponential growth. However, extracellular AZA in the supernatant after gentle centrifugation could be up to >50% depending on strain and growth conditions. In the present study the ratio of AZA in the cell pellet and supernatant was approximately 3:7 including potential cell lysis during the more disruptive continuous flow centrifugation.

Both methanol eluates were dried under vacuum on a small amount of silica gel and directly loaded onto a Si 60 column (320×25 mm, 40–63 μm, Merck, Germany). Compounds were eluted at 5 mL min^{-1} by stepwise elution (20% increments) from 100% hexane to 100% ethyl acetate to 100% methanol. All azaspiracid-containing fractions were pooled and subjected to LC reversed-phase purification on a Waters Alliance 2695 with photodiode array detection (230 nm) on a C18 column (150 × 10 mm, 5 μm, Machery & Nagel, Düren, Germany) with solvent A: water with 2 mM ammonium acetate, and solvent B: methanol with 2 mM ammonium acetate. Elution was performed with a stepwise gradient starting with at 50:50 A and B for 10 min, followed by a 30 min gradient to 100% B and held for 10 min. The column was washed for 10 min with 100% AcN after each injection and then re-equilibrated to 50:50 A:B over 10 min. A final HPLC purification step was performed at 1 mL min^{-1} with solvent A: water with 4 mM ammonium formate and solvent B: AcN with 4 mM ammonium formate on an ISIS C18 column (4.6 mm × 250 mm, 5 μm, Machery & Nagel, Düren, Germany). Elution

was performed isocratically at 55% solvent B for 10 min followed by a wash step with 100% B for 3 min and re-equilibration to 55% B over 10 min. Salt and buffer were removed using a SPE cartridge (500 mg, C18 endcapped, Chromabond, Machery & Nagel, Düren, Germany). Purity of toxins was determined by NMR spectroscopy (see below) as well as LC-MS. For bioactivity assays, 250 μg for the in vivo experiments and 20 μg for the in vitro experiments were sealed in combusted ampules (Wheaton, Sigma-Aldrich, Taufkirchen, Germany) under argon atmosphere.

2.2. LC-MS/MS quantification and HRMS/MS

Quantification by liquid chromatography-tandem mass spectrometry (LC-MS/MS) was performed in selected reaction monitoring mode on a triple quadrupole mass spectrometer (API 4000 QTrap, Sciex, Darmstadt, Germany) equipped with a TurboSpray interface and coupled to an HPLC (degasser G1379A, binary pump G1311A, autosampler G1330B, column oven G1316A, all Agilent, Waldbronn, Germany). Chromatography was achieved using a reverse-phase analytical C8 column (Hypersil BDS 120 Å, 50×2 mm, 3 μm, Phenomenex, Aschaffenburg, Germany) at 20 °C with a flow-rate of 0.2 mL min^{-1} as previously described by Kim et al. (2017). Gradient elution was performed with two eluents, where eluent A was water and eluent B was AcN/water (95:5 v/v), both containing 2.0 mM ammonium formate and 50 mM formic acid. Initial conditions were 8 min column equilibration with 30% B, followed by a linear gradient to 100% B in 8 min, and isocratic elution for 10 min with 100% B. The system was then returned to initial conditions. Mass transition used for quantification were *m/z* 842>824 (min 2.25) and *m/z* 860>842 (min 1.65) for AZA-1 and AZA-59, respectively, and acquired under the following conditions: curtain gas: 10 psi, CAD: medium, ion spray voltage: 5500 V, temperature: ambient, nebulizer gas: 10 psi, auxiliary gas: off, interface heater: on, declustering potential: 100 V, entrance potential: 10 V, exit potential: 30 V. Dwell time was 20 ms and collision energy 40 V for both transitions. Confirming daughter ions for the group 4 and group 5 fragments are identical for both compounds (AZA-59: *m/z* 860>362, 860>262, AZA-1: *m/z* 842>362, 842>262).

Accurate mass characterization of AZA-59 was achieved using syringe (500 μL Hamilton) direct infusion at 15 μL min^{-1} on a QExactive Plus mass spectrometer (Thermo Fisher Scientific, Bremen, Germany) equipped with a heated electrospray ionization (HESI-II) source. The mass spectrometer was calibrated (*m/z* 138.06619 to *m/z* 1621.96509) using Positive Ion Calibration Solution (Pierce, Thermo Fisher Scientific). HRMS measurement were (sequentially) performed in HCD fragmentation mode at 15, 30, 40, 55 and 65 NCE (Figure S1) with a resolution of 280,000, a scan range of 125 to 900 *m/z,* automatic gain control of 10^6, 50 ms maximum injection time, in positive mode using a spray voltage of 3.5 kV.

2.3. NMR analyses

Purified AZA-59 was dried under vacuum and dissolved in 40 μL deuterated methanol (3.33 ppm of residual CHD_2OD for ^1H NMR and 49.0 ppm for ^{13}C). BRUKER standard pulse programs as well as IMPACT-HMBC (Furrer, 2010) were used. NMR experiments were measured at 292 K with an AVANCE II 600 MHz NMR spectrometer equipped with a 1.7 mm CPTCI cryoprobe (all Bruker, Rheinstetten, Germany). The spectra were referenced to the solvent residual peak. Dried samples of AZA-59 were dissolved in 60 μL deuterated methanol containing 5.78 mmol L^{-1} 1,4-dioxane, confirmed by external calibration, and transferred to a 1.7 mm NMR tube for quantification. Proton spectra were acquired with ns = 32, aq = 3 s and d1 = 17 s.

2.4. In vitro Jurkat T lymphocyte cytotoxicity assay

Human Jurkat E6–1 T lymphocyte cells (American Type Culture Collection TIB-152; Manassas, VA, USA) were cultured as described in Twiner et al. (Twiner et al., 2005, 2012b). Briefly, cells were grown in RPMI-1640 medium supplemented with 10% (v/v) fetal bovine serum (FBS), 1.0×10^{-2} M L-glutamine, 1.0×10^{-4} g mL^{-1} penicillin and 1.0×10^{-4} g mL^{-1} streptomycin at 37 °C in a humidified 95% air/5% CO_2 atmosphere. Cells were 1:4 sub-cultured with fresh medium twice a week. All cell reagents were purchased from Sigma-Aldrich (Milan, Italy). Cell viability was measured by the MTS [3-(4,5-dimethylthiazol-2-yl)-5-(3-carboxymethoxyphenyl)-2-(4-sulfophenyl)-2*H*-tetrazolium] assay (CellTiter 96® Aqueous One Solution Cell Proliferation Assay; Promega; Milan, Italy). Briefly, 3×10^4 cells $well^{-1}$ were seeded in round bottom 96-well plates, in 200 μL cell medium. After 24 h culture, cells were exposed to AZA-1 or AZA-59 (10^{-12} – 10^{-7} M) for 24, 48, and 72 h. Then, 10 μL MTS (1:20) solution were added to the cells which were incubated for 4 h. Cell viability was quantified measuring the absorbance at 492 nm, using a microplate reader (FLUOstar Omega; BMG Labtech; Ortenberg, Germany). Cell viability is expressed as % of control (cells not exposed to the toxins) and presented as means ± standard error (S.E.) of three independent experiments performed in triplicate.

2.5. Acute intraperitoneal toxicity in mice

2.5.1. Toxins

AZA-59 (250 μg) used in these experiments was produced as part of this study. AZA-1 (250 μg) used for comparison was produced as part of the ASTOXII project (previously described by Kilcoyne et al., 2012).

2.5.2. Animals

Female CD-1 mice (20–22 g) were purchased from Envigo Rms S.r.l. (San Pietro al Natisone, Udine, Italy). Animals were acclimatized for 2 weeks before the experiments, at controlled temperature (21 ± 1 °C) and humidity (60–70%), under a fixed artificial light cycle (07.00–19.00). Mice were caged in groups of 3 to 9 animals, using dust free poplar chips for bedding and fed a standard diet for rodents. Feed and water were provided ad libitum during all phases of the study.

2.5.3. Permits

Animal experiments were carried out at the University of Trieste in compliance with the Italian D.L. n. 26 of 4th March 2014 and associated guidelines in the European Union on the protection of animals used for scientific purposes (Directive 2010/63/EU of the European Parliament and of the Council of 22nd September 2010). Experiments were approved by the University Body for Animal Well-being (OPBA) of the University of Trieste and by Italian Ministry of Health (authorization n° 106/2020-PR).

2.5.4. Experimental design

Mice were weighed immediately before treatment. AZA-1 or AZA-59, dissolved in phosphate buffered saline (PBS) pH 7.0 containing 1.8% (v/v) ethanol, were injected intraperitoneally to groups of 5 to 9 mice (administered volume: 10 mL kg^{-1} body weight). Each toxin was administered following the four-dose response surface design (Fig. 1) as detailed in Aune et al. (2007) (5 mice at level 1, 5 mice at level 2, 7 mice at level 3, and 9 mice at level 4). The starting dose of AZA-1 or AZA-59 (level 1) were 100 or 300 μg kg^{-1}, respectively, and the subsequent doses (levels 2–4) were progressively decreased if lethality was higher than 50% at the previous dose level, or increased if it was lower than 50% (Fig. 1). These starting doses were chosen based on the previously established toxicity of AZA-1 (74 μg kg^{-1}; Kilcoyne et al., 2014a) and the assumption that AZA-59 would be approximately 3-fold less potent compared to AZA-1. This assumption was based on both the initial *in-vitro* studies on Jurkat T lymphocytes as well as structural similarities to AZA-37, which was previously found to be 3-fold less potent compared to AZA-1 toward Jurkat T cells (Krock et al., 2015). In parallel to each dose level, groups of 3 control mice were administered with the vehicle alone (10 mL kg^{-1} body weight).

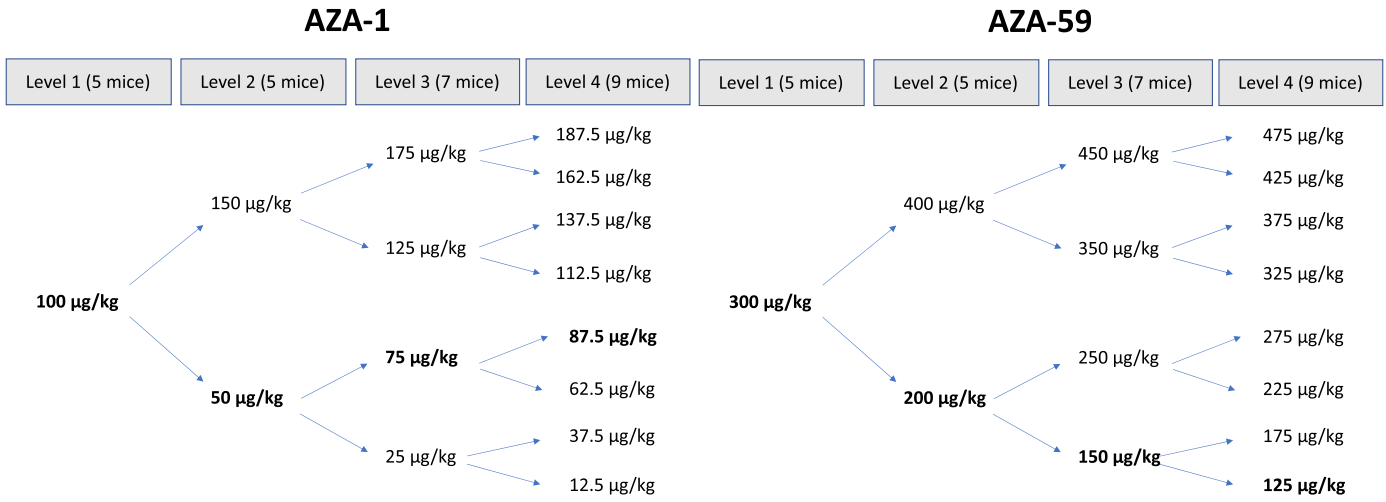

Fig. 1. Four level design to evaluate the acute i.p. toxicity of AZA-1 and AZA-59. The obtained pathway based on lethality recorded at each dose level is highlighted in bold.

After treatment, mice were observed for 24 h, recording mortality and signs of toxicity. Then, mice were weighed and anesthetized by intraperitoneal injection of tiletamine/zolazepam (Zoletil®; Virbac; Milan, Italy; 20 mg kg^{-1}) and xylazine (Virbaxyl®; Virbac; Milan, Italy; 5 mg kg^{-1}) and exsanguinated. After necropsy, the main organs and tissues were removed and fixed in neutral buffered 10% formalin for the histological analysis. Similarly, mice which died during the observation period were immediately weighed and necropsied; the main organs and tissues were removed and fixed for histological analysis.

2.5.5. Histological analysis

Heart, lungs, thymus, liver, kidneys, spleen, stomach, duodenum, jejunum, colon, rectum, pancreas, cerebrum, cerebellum, uterus and ovaries, fixed in 10% neutral buffered formalin, were dehydrated, embedded in paraffin and cut in sections of 5 µm. Sections were stained with hematoxylin-eosin and submitted to a blind histopathological examination. Pictures were obtained by an inverted light Leica DMi1 microscope equipped with a FLEXACAM C1 standard camera (Leica Microsystems; Milan, Italy).

2.6. ELISA

ELISA measurements were conducted according to Samdal et al. (2019). Reagents and organic solvents were reagent grade or better. Reference AZA-1 was CRM-AZA-1 from NRC (Halifax, NS, Canada). Briefly, maxisorp immunoplates (Nunc, Roskilde, Denmark) were coated overnight with OVA−cdiAZA1, blocked with 1% PVP, incubated with standards and antiserum AgR 367–11b followed by donkey antisheep IgG-HRP (Agrisera, Vännäs, Sweden) and finally the color was developed with HRP-substrate K-blue Aq. (Neogen, Lexington, KY, USA) and stopped with 10% H_2SO_4. Absorbance was measured at 450 nm using a SpectraMax i3x plate reader (Molecular Devices, Sunnyvale, CA, USA). The toxins were three-fold diluted in the sample buffer, giving 10 standards from 0.007–131 ng mL^{-1} (AZA-1) and 0.0050–100 ng mL^{-1} (AZA-59), respectively. Two technical replicates from each standard and concentration were averaged and the measurement was repeated over three different plates/days. Assay standard curves were calculated using 4-parameter logistic treatment of the data using SoftMax Pro-version 6.5.1. (Molecular Devices, Sunnyvale, CA, USA). Cross-reactivity of AZA-59 was calculated in comparison to AZA-1 according to Samdal et al. (2015; 2019). To account for the difference in molecular weight (Mw), concentration at 50% inhibition/competition (I_{50} in ng mL^{-1}) was converted using I_{50} (Mw) [nM] = (I_{50} /Mw). Cross reactivity values for AZA-59 are reported relative to the I_{50} of the AZA-1 CRM. Percentage cross-reactivity was calculated as the mean I_{50} (Mw) value for AZA-1 divided by the mean I_{50} (Mw) value for AZA-59 and multiplying by 100. Intra-assay variation was calculated based on 3 competition curves as follows: CV (%) = 100 × (standard deviation of I_{50})/(mean of I_{50}).

2.7. Statistics

Data are expressed as mean ± standard deviation (S.D.). Significant differences between control and experimental groups were calculated by one-way analysis of variance, followed by the Dunnett's test for multiple comparisons of unpaired data, accepting $p < 0.05$ as significant. LD_{50} (in vivo i.p. lethal dose for 50% of the treated mice), based on 24 h mortality data, was calculated according to the Finney method at a 95% confidence level (Finney, 1971), using Elsevier-Biosoft software (Cambridge, UK). For the in vitro cytotoxicity on Jurkat E6–1 T lymphocytes, IC_{50} values (concentration inhibiting cell viability by 50%) were calculated by four-parameter linear regression using the GraphPad Prism v.6 software (GraphPad Prism Inc.; San Diego, CA, USA), at a statistical confidence interval of 95%. Statistical analysis was performed by two-way analysis of variance, using the GraphPad Prism v.6 software (GraphPad Prism Inc.; San Diego, CA, USA) and significant differences were considered for p values < 0.05.

3. Results

3.1. Purification and structure elucidation

Mass culturing and subsequent purification of AZA-59 yielded approximately 275 µg of pure toxin. High resolution mass spectrometry of AZA-59 (Table 1, Figure S1, Table S1) showed a fragmentation analogous to AZA-37 (Fig. 2B). The sum formulas of the HRMS daughter ions for AZA-59 (Table 1, Table S1) showed a difference of CH_2 in the I ring in comparison to AZA-37 (Krock et al., 2015) or additional oxygen between C1 and C8 in comparison to AZA-1 (Fig. 2A). The *m/z* 798 fragment (Table 1) also suggested a hydroxyl group at C3 as well as a 4, 5-olefin (Sandvik et al., 2021). Nuclear magnetic resonance spectroscopy (NMR) only showed discrepancies in the spectra for the nuclei of ring I in comparison to AZA-37 (Krock et al., 2015) (Fig. 2C, C38 to C40, Table S3, Figure S3-S13). C39 in AZA-59 gave a signal indicative for a CH-group (135° DEPT, Figure S5) in contrast to the CH_2-group in AZA-37. Discrepancies in comparison to spectra of AZA-1 were found for the proton at C3 and two CH_2 signals at C7 and C8, respectively. The absolute stereochemistry of AZA-59 could not be determined by NMR. However, 37-*epi*-AZA-1 (Kilcoyne et al., 2014b) clearly showed a strong

Table 1
Observed and theoretical mass-to-charge (m/z) ratios, relative intensity, elemental composition, and deviation from the calculated mass in ppm for AZA-59 at 40 NCE (Figure S1, extended mass list Table S1).

Formula $[M+H]^+$	Measured $[m/z]$	Calculated $[m/z]$	Δ [ppm]	Rel.int. [%]
$C_{47}H_{74}NO_{13}$	860.51527	860.51547	-0.22	6.1
$C_{47}H_{72}NO_{12}$	842.50490	842.50490	-0.06	100
$C_{46}H_{72}NO_{10}$	798.51479	798.51507	-0.36	9.35
$C_{40}H_{62}NO_9$	700.44200	700.44191	0.14	14.2
$C_{40}H_{60}NO_8$	682.43140	682.43134	0.09	10.5
$C_{27}H_{44}NO_5$	462.32147	462.32140	0.15	19.7
$C_{22}H_{36}NO_3$	362.26894	362.26897	-0.08	36.0
$C_{16}H_{24}NO_2$	262.18021	262.18016	0.32	5.5
$C_{10}H_{18}NO$	168.13836	168.13829	0.38	16.2

effect of the stereochemical configuration at C-37 on proton shifts in ring H and I in comparison to AZA-1. Such a shift was not observed for AZA-59 (Table S3), therefore, the same relative stereochemical configuration of AZA-1 and 59 in ring H and I is likely. Further, the polyclonal antibodies used in ELISA are specific for C26-C40 region of AZA-1. The similar cross reactivity of AZA-1 and AZA-59 (see below) also suggests that both molecules share the same stereochemistry between C26-C40. In summary, the structure of AZA-59 (Fig. 2C) was confirmed as a C39-methyl analogue of AZA-37 or the C3-hydroxyl, C7–C8 saturated double bond analogue of AZA-1 (Fig. 2A) with the same stereochemistry between C26-C40 in comparison to AZA-1 (Satake et al., 1998b; Ofiji et al., 1999; Nicolaou et al. 2003a,b; Nicolaou et al. 2004 a,b; Kenton et al. 2018a,b).

3.2. In vitro cytotoxicity of AZA-59 and AZA-1

The relative cytotoxic potency of AZA-59 in comparison to AZA-1 was determined using a Jurkat T lymphocyte model which is sensitive to subnanomolar–submicromolar concentrations and gives insight into the structure-activity relationship of AZAs and target proteins (Krock et al., 2015; Kilcoyne et al., 2014c, 2018; Twiner et al., 2005, 2012b, 2012c). Cells viability was evaluated after 24, 48 and 72 h exposure to each toxin at concentrations ranging from 10^{-12} to 10^{-7} M (Fig. 3). After 24 h, the two toxins exerted a similar effect, inducing only a slight reduction of cell viability at the highest concentration (10^{-7} M). AZA-59 and AZA-1 reduced cell viability to 69% and 68%, respectively. The cytotoxic effect of AZA-59 and AZA-1 increased after 48 h exposure, AZA-59 being slightly less potent than AZA-1. A similar effect was recorded after 72 h exposure, with AZA-59 inhibiting cell viability by 50% (IC_{50}) at a concentration of 2.6×10^{-9} M (95% Confidence Interval, CI = 1.5–4.4 × 10^{-9} M). The cytotoxic effect of AZA-59 was ~5-fold lower ($p < 0.001$) than that of the reference toxin AZA-1 ($IC_{50} = 5.1 \times 10^{-10}$ M; 95% CI = 2.4 – 10.7 × 10^{-10} M).

3.3. Acute intraperitoneal toxicity of AZA-59 and AZA-1 in mice

3.3.1. Lethality and clinical signs

Lethality data and clinical signs of mice within 24 h after i.p.

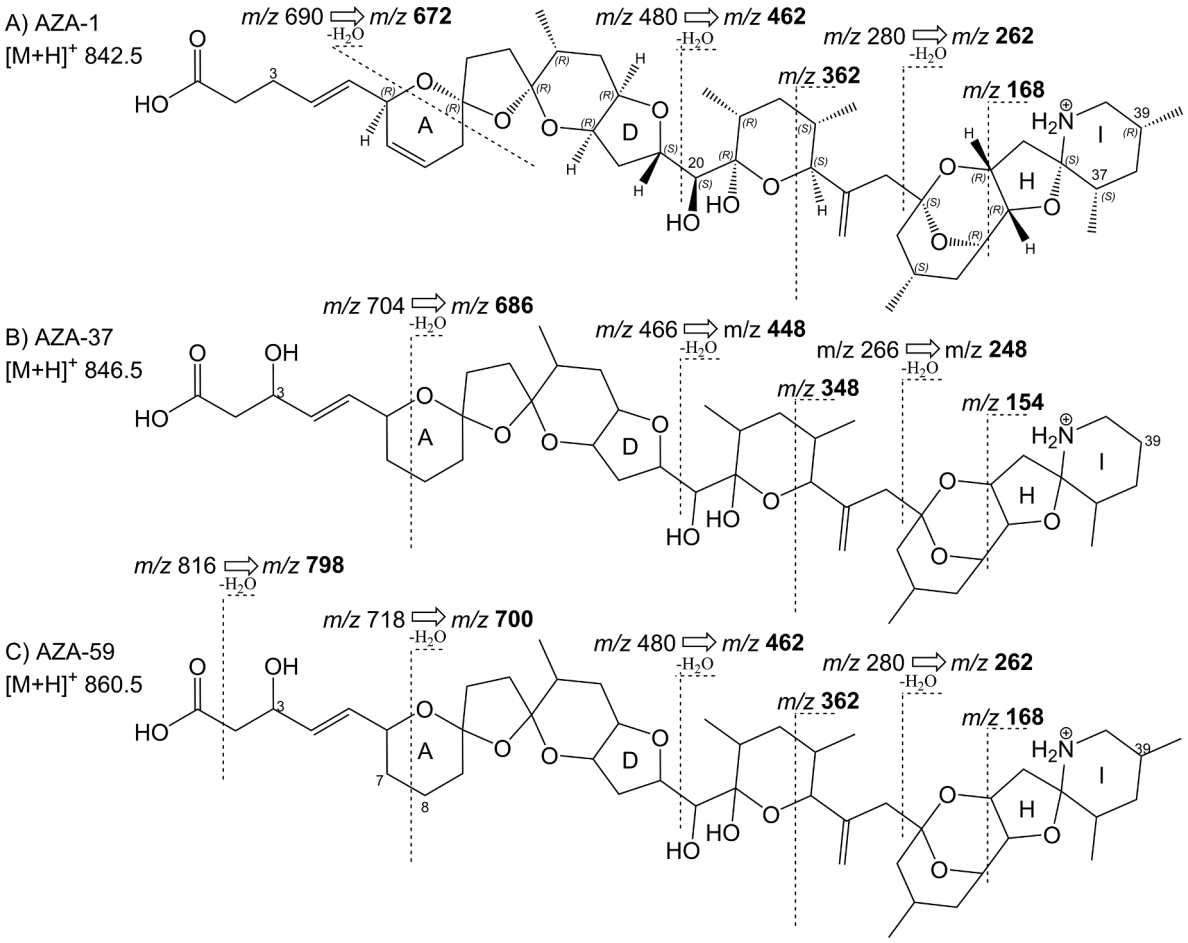

Fig. 2. Structures of A) AZA-1 Satake et al., 1998b; revised by Nicolaou et al. 2003a,b, 2004 a,b; Kenton et al. 2018a,b), B) AZA-37 (Krock et al., 2015), and C) AZA-59, all with characteristic mass spectrometry fragmentation cleavages and observed m/z values for the daughter ions (bold print). All structures are depicted as the $[M + H]^+$ ion.

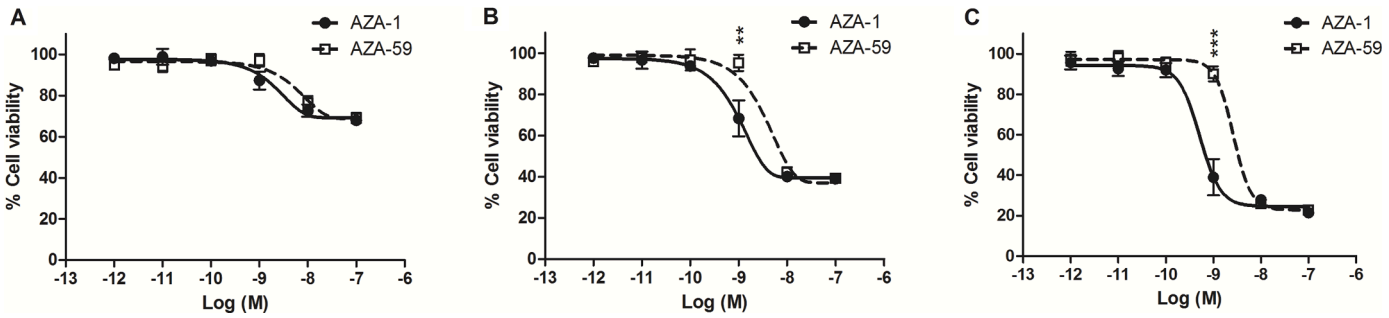

Fig. 3. Cytotoxicity for AZA-59 and AZA-1 toward Jurkat T lymphocytes after 24 h (A), 48 h (B), and 72 h (C) exposure as determined by the MTS assay. Data are the mean ± S.E. of 3 independent experiments and expressed as relative % viability to untreated control cells (equal to 100%). Statistical analysis: **, $p < 0.01$; ***, $p < 0.001$ (two-way analysis of variance and Bonferroni's post-test, between AZA-1 and AZA-59).

Table 2
Lethality and signs of toxicity in mice within 24 h from AZA-59 or AZA-1 i.p. injection.

Group of treatment	Dose (μg kg^{-1})	Lethality[a]	Survival times mice that died during the assay (h:min)	Signs of toxicity
Controls	–	0/18	–	–
AZA-59	75.0	0/9	–	Reduced motor activity
	87.5	3/9	11:16 - 12:05 – 23:20	Reduced motor activity, lethargy, dyspnea, spasms
	125.0	9/9	02:05 – 02:24 - 03:45 – 03:46– 03:47 – 03:47 –03:49 – 09:46 –10:00	Reduced motor activity, lethargy, dyspnea, spasms
	150.0	4/7	05:43 – 06:25 – 06:34 – 07:18	Reduced motor activity, lethargy, dyspnea, spasms
	200.0	4/5	02:02 – 02:09 – 02:13 – 02:38	Reduced motor activity, lethargy, dyspnea, spasms
	300.0	4/5	00:45 – 01:05 – 01:10 – 01:25	Reduced motor activity, lethargy, dyspnea, spasms
AZA-1	50.0	0/5	–	Reduced motor activity, lethargy
	75.0	2/7	10:37 – 23:36	Reduced motor activity, lethargy, dyspnea, spasms
	87.5	4/9	09:07 – 12:18 – 22:34 – 22:37	Reduced motor activity, lethargy, dyspnea, spasms
	100.0	3/5	11:55 – 12:00 –23:45	Reduced motor activity, lethargy, dyspnea, spasms

[a] Number of animals that died/total number of treated animals.

injection of AZA-59 or AZA-1 are reported in Table 2. At the first dose level, AZA-59 (300 μg kg^{-1}) was lethal for 4/5 (80%) mice, and the same effect was recorded reducing the dose level 2 to 200 μg kg^{-1} (lethality: 4/5 mice, 80%). The third dose level was reduced to 150 μg kg^{-1} and caused the death in 4/7 (57%) mice, whereas further reduction of the fourth dose to 125 μg kg^{-1} resulted in 9/9 (100%) dead mice. Thus, to calculate the LD_{50} of AZA-59, additional groups of 9 mice were injected with the toxin at 87.5 and 75 μg kg^{-1} (dose levels 4 and 5), which caused the death of 3/9 (33%) and 0/9 (0%) mice respectively. At the first dose level, AZA-1 (100 μg kg^{-1}) induced the death of 3/5 (60%) mice, whereas the second dose level reduced to 50 μg kg^{-1} was not lethal for 5 injected mice. The third dose level was then increased to 75 μg kg^{-1} recording 2/7 (29%) dead mice, while the fourth dose level increased to 87.5 μg kg^{-1} was lethal for 4/9 (44%) mice. Based on 24 h lethality data, the i.p. LD_{50} of AZA-59 was 122 μg kg^{-1} (95% confidence limits, CL: 91–165 μg kg^{-1}), higher, though not significantly different ($p = 0.115$), than that of AZA-1 (LD_{50} = 92 μg kg^{-1}; 95% CL: 79–107 μg kg^{-1}). Considering AZA-1 as reference toxin, the TEF of AZA-59 derived from LD_{50} values is 0.8. The death of more mice (9/9) after injection of 125 μg kg^{-1} of AZA-59 in comparison to 200 μg kg^{-1} (4/5) and 300 μg kg^{-1} (4/5) was likely due to inter-individual sensitivity, as observed previously for other phycotoxins, and was not significant ($p>0.05$).

Mice administered with AZA-59 or AZA-1 showed a reduced motor activity, even at their non-lethal dose. Moreover, after lethal doses administration, mice became lethargic, laying with sternal recumbency, and with dyspnea and spasms of the hind limbs before death (Table 2).

3.3.2. Necropsy

Necropsy showed macroscopic alterations in the internal organs of mice that died during the assay as well as those sacrificed 24 h after AZA-59 injection (Table 3). In particular, mice that died ~ 5 h or more after the toxin injection and those sacrificed after 24 h presented with an enlarged pale liver. Liver weight significantly increased (17–45%) after each dose administration, in comparison to controls. Mice that were injected with 75–200 μg kg^{-1} AZA-59 displayed a significant reduction (17–27%) of the spleen weight (Table 3). Other macroscopic findings include redness of the lungs (2/9, 1/9, 3/7 and 1/5 mice treated with the doses of 87.5, 125, 150 and 300 μg kg^{-1}, respectively), which was not dose-related (data not shown). Similar macroscopic changes were also observed in mice that died during the assay and in those sacrificed 24 h after AZA-1 injection. Specifically, the weight of liver increased (24–41%, as compared to controls) and the weight of the spleen decreased (32–34%, as compared to controls). No significant differences were recorded between mice administered with the same doses of AZA-59 or AZA-1.

3.3.3. Histopathology

Histological analysis showed that i.p. injection of AZA-59 or AZA-1 caused tissue changes in the liver, pancreas, thymus, and spleen. These alterations were recorded at all the administered doses, both in mice that died during the observation period and in those that survived up to 24 h. In particular, hepatocellular changes consisted of a reduced glycogen content in hepatocytes, which were swollen and less stained than those of the control mice. The liver parenchyma was characterized by the presence of degenerating cells, including apoptotic ones, which were vacuolated, in some mice even with macrovacuoles (Fig. 4). The exocrine pancreas of mice injected with AZA-59 or AZA-1 showed degenerated cells characterized by vacuolated swelling, mainly in the peripheral parts of the lobuli (Fig. 5A–C). The cortex of thymus showed the presence of apoptotic cells and clear spaces containing cellular debris (Fig. 5D–F). An increased number of apoptotic cells was also noted in the spleen (data not shown).

3.5. Quantification of AZA-59 by ELISA and LC-MS/MS in comparison to AZA-1

An established ELISA method that detects a wide range of structural AZA analogues was used (Samdal et al., 2015, 2019) to test its ability to

Table 3
Weight of mouse liver and spleen within 24 h after AZA-59 or AZA-1 i.p. injection.

Group of treatment	Dose (μg kg^{-1})	Number of mice	Liver (mg) Mean ± S.E.	Spleen (mg) Mean ± S.E.
Controls	–	15	1296.5 ± 40.1	100.3 ± 3.5
AZA-59	75.0	9	1826.0 ± 99.2** *(+41%)*	74.1 ± 4.2** *(- 26%)*
	87.5	9	1884.3 ± 128.5** *(+45%)*	72.9 ± 3.8** *(- 27%)*
	125.0	9	1512.5 ± 47.6* *(+17%)*	86.3 ± 5.5* *(- 14%)*
	150.0	7	1521.2 ± 95.3* *(+17%)*	82.3 ± 7.2* *(- 18%)*
	200.0	5	1617.4 ± 93.2* *(+25%)*	83.0 ± 5.6* *(- 17%)*
	300.0	5	1515.2 ± 73.2* *(+17%)*	95.7 ± 7.7 *(- 5%)*
AZA-1	50.0	5	1604.9 ± 85.4** *(+24%)*	66.5 ± 3.4** *(- 34%)*
	75.0	7	1794.1 ± 108.4** *(+38%)*	66.1 ± 6.5** *(- 34%)*
	87.5	9	1606.5 ± 99.3* *(+24%)*	68.5 ± 5.6** *(- 32%)*
	100.0	5	1659.8 ± 88.6** *(+28%)*	67.7 ± 6.5** *(- 33%)*

* $p < 0.05$.
** $p < 0.001$ at the analysis of variance, as compared to controls; no significant differences were recorded between mice administered with AZA-59 or AZA-1, at the same doses; in brackets: % difference to controls.

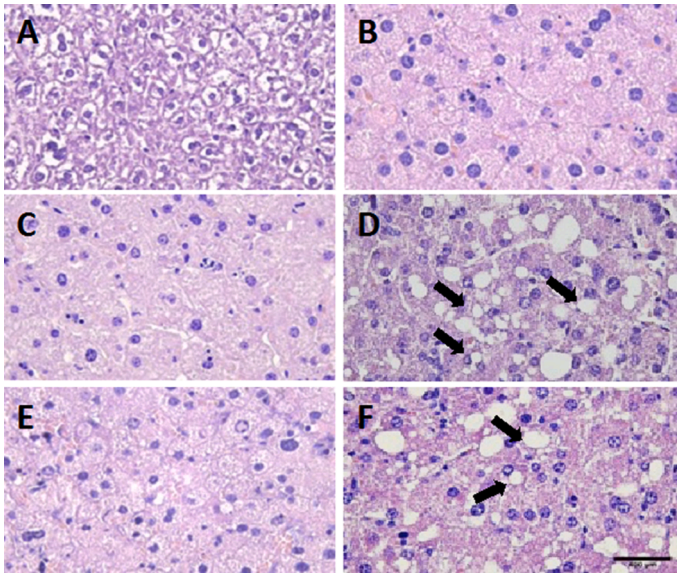

Fig. 4. Representative light micrographs of the liver from a control mouse (A) and from mice intraperitoneally injected with 87.5 μg kg^{-1} AZA-59 (B-D) or AZA-1 (E, F), all stained with haematoxylin–eosin. Arrows indicate cells with macrovacuoles. Original objective magnification: 40x); scale bar: 400 μm.

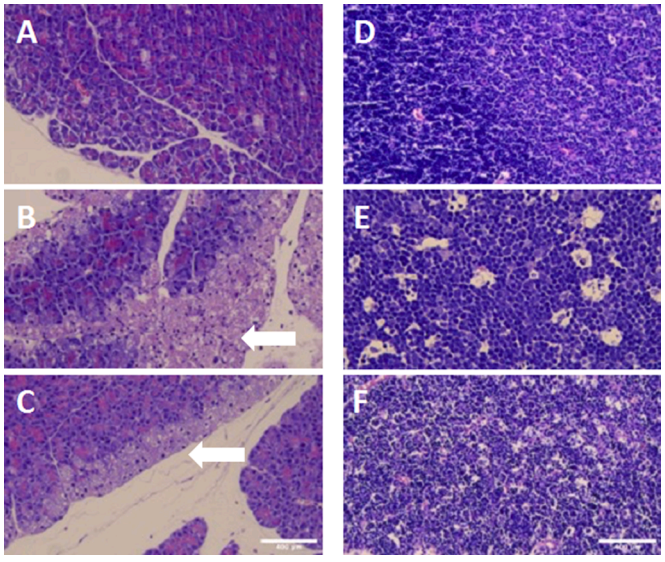

Fig. 5. Light micrographs of the pancreas (A–C) and thymus (D–F) from a control mouse (A and D) and from mice intraperitoneally injected with 87.5 μg kg^{-1} AZA-59 (B and E) or AZA-1 (C and F), all stained with haematoxylin–eosin. Arrows indicate altered cells of pancreatic lobuli. Original objective magnification: 20x); scale bar: 400 μm.

detect and quantify AZA-59. The competitive binding of the polyclonal antibodies had statistically the same cross reacivity for AZA-59 in comparison to AZA-1 (Table 4). This suggested, that the structural differences between both analogues do not effect detection and quantification using the AZA ELISA and that AZA-1 can be utilized as a reference standard in the absence of available AZA-59 reference standards.

The response factor of AZA-59 was also compared with AZA-1 by LC-MS/MS analyses, using the first water loss transition of both molecules as the quantitative ion. The linear regression for the calibration curves of AZA-59 (*m/z* 860>842) and AZA-1 (*m/z* 842>824) standards in methanol were very similar independent if the standard concentration was compared as molar concentration (Fig. 6) or pg μl^{-1} (Figure S2). Consequently, AZA-59 concentrations calculated from the peak area and the calibration curve equation of AZA-1 were similar to the concentration when calculated from the AZA-59 calibration equation (Table S2). The largest relative deviation of calculated and expected concentrations were found for the lower concentrated standards (0.84–6.68 fmol μL^{-1}) that were relatively overestimated via the AZA-1 calibration equation and underestimated via the AZA-59 calibration equation, respectively (Table S2). These differences were, however, most likely due to the larger analytical standard deviation for the low concentrated standards and not a systematic ionization difference between AZA-59 and AZA-1. Therefore, AZA-1 could serve as a good analytical reference standard to approximate the concentration of AZA-59 until certified standards become available. However, instrument specific variances, differences between other mass transitions as well as matrix effects or interference of potential co-elutants have to be evaluated during a controlled laboratory ring-trial.

4. Discussion

Structural analyses confirmed AZA-59 (Fig. 2C) as the C3-hydroxyl, C7–C8 saturated double bond analogue of AZA-1 (Fig. 2A) or the C39-methyl analogue of AZA-37 (Fig. 2B). The in vivo toxicity results showed that, within 24 h from i.p. injection, the lethal potency of AZA-59 was lower than that of AZA-1, with a median lethal dose (LD_{50}) of 122 μg kg^{-1} (95% CL: 91–165 μg kg^{-1}) and 92 μg kg^{-1} (95% CL: 79–107 μg kg^{-1}), respectively. Although the differences were not statistically significant at this level of replication, LD_{50} values were used to calculate a provisional TEF for AZA-59, equal to 0.8 (reference AZA-1 defined as 1.0), accordingly to the approach reported by EFSA in deriving the TEFs of other AZAs from their acute intraperitoneal lethal dose (EFSA, 2008).

Table 4
Mean molar cross-reactivities of AZA-59 in comparison to AZA-1.

Toxin	Start conc. [ng mL^{-1}]	Molecular weight (Mw) [g mol^{-1}]	n	I_{50}[a] [ng mL^{-1}]	I_{50} (Mw)[d] [nM]	%CV[e]	%CR[b]
AZA-1[c]	130.696	842.06	3	1.419	1.685	20	100
AZA-59	100.000	860.08	3	1.202	1.397	22	121

[a] I_{50} is the concentration of analogue giving 50% inhibition of binding of antibody to the coating antigen (OVA-cdiAZA1).
[b] Molar cross-reactivity;% CR = 100 × (I_{50} AZA-1)/(I_{50} analogue).
[c] NRC CRM 0571 (2006).
[d] I_{50} (Mw) [nM] = (I_{50} /Mw).
[e] CV is the Intra-assay variation.

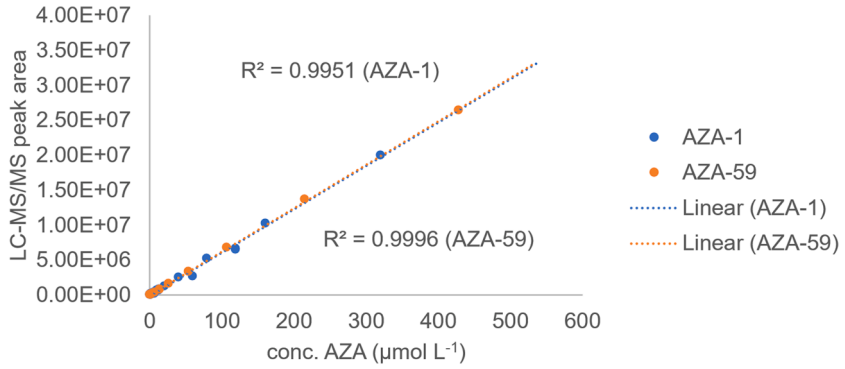

Fig. 6. Calibration curves for standard dilution series of AZA-59 and AZA-1 (concentration determined by qNMR and dilution calculation). The area for the transition of the first water loss (AZA-59: *m/z* 860>842, AZA-1 *m/z* 842>824) are shown.

After i.p. injection, mice showed reduced motor activity and lethargy, followed by dyspnea and spasms in the hind limbs in mice that died. Similar symptoms were previously observed in mice after i.p. injection of mussel extracts containing AZAs (Twiner et al., 2008) as well as after single oral administration of AZA-1, AZA-2, or AZA-3 (Pelin et al., 2018).

Necropsy showed swollen pale liver in mice that died during the assay and those sacrificed 24 h after AZA-59 or AZA-1 administration. This was consistent with the observed significant weight increase of the liver (17–45% and 24–41%, after AZA-59 and AZA-1 injection, respectively). A hepatotoxic effect of AZA-59 and AZA-1 was also observed by light microscopy showing swollen vacuolated hepatocytes even in mice administered with the non-lethal dose of AZA-59 or its analogue. Liver changes were also reported in response to single oral administration of AZA-1, AZA-2, or AZA-3 (Ito et al., 2000; Pelin et al., 2018), indicating an acute hepatotoxic effect of these toxins independent of their route of administration. Ito et al. (2000, 2002) associated the liver color change with lipids accumulation in hepatocytes. Necropsy also showed tissue alterations in the exocrine pancreas of mice treated with AZA-59 or AZA-1. In particular, degenerated cells were mainly observed in the peripheral parts of the pancreatic lobules. These cells were characterized by a vacuolated swollen aspect suggesting a hydropic degeneration induced by the toxins, as previously reported for partially purified AZA-1 (Ito et al., 1998).

AZA-59 and AZA-1 also affected the spleen and the thymus. A significant reduction of spleen size and weight (17–27%) was recorded in mice treated with AZA-59 which died after more than 2 h from toxin administration or were sacrificed at 24 h, i.e., those administered with the doses of 75–200 µg kg^{-1} and the single surviving mouse which received the highest dose (300 µg kg^{-1}). The reference toxin AZA-1 induced ~30% reduction of the spleen weight across all tested doses. Light microscopy showed increased numbers of apoptotic cells in the spleen, suggesting AZA-59 and AZA-1 toxicity towards the lymphoid elements previously reported recorded after single oral administration of AZA-1 and some of its analogues in mice (Ito et al., 2000; Pelin et al., 2018) and after AZA-1 repeated oral administration (Ito et al., 2002). Light microscopy also showed tissue change in the thymus cortex, visible as apoptotic cells and clear spaces containing cellular debris consistent with earlier findings for partially purified AZA (Ito et al., 1998). Thus, lymphoid organs appear to be affected by AZAs in general. No differences were observed compared to control mice for heart, lungs, kidneys, stomach, duodenum, jejunum, colon, rectum, cerebrum, cerebellum, uterus, or ovaries.

The cytotoxic effect of AZA-59 and AZA-1 toward lymphocytes is supported by the in vitro study on Jurkat cells, which are sensitive to subnanomolar–submicromolar concentrations of AZAs (Krock et al., 2015; Kilcoyne et al., 2014c, 2018; Twiner et al., 2005, 2012b, 2012c). The MTS assay, that evaluates the mitochondrial activity in viable cells, showed a clear concentration- and time-dependent cytotoxic effect of AZA-59 on Jurkat cells. The concentration of AZA-59 that reduced cell viability by 50% (IC_{50}) after 72 h exposure was 2.6 × 10^{-9} M, corresponding to ~5-fold lower cytotoxic potency in comparison to AZA-1 (IC_{50} = 5.1 × 10^{-10} M). Cytotoxicity has been estimated for a number of AZA analogues (Table 5). AZA-59 showed ~5-fold lower cytotoxicity compared to AZA-1 similar to lower toxicities found for AZA-33, -36, and -37. Other AZAs such as AZA-2, -3, and -34 are significantly higher in cytotoxicity compared to AZA-1. However, no clear trends in structure-activity relationships emerge from this data. AZA-59 showed reduced toxicities in comparison to AZA-1, indicating that the double bond in ring A and/or hydroxyl group at C-3 (Fig. 1) is an important toxicity feature. 37-*epi*-AZA-1, on the other hand, only differs in the stereochemistry at C-37 in comparison to AZA-1 but shows 5-fold higher toxicity (Kilcoyne et al., 2014b), underlining the role of ring I. AZA-37 and -59 differ in the methyl group at C-39 but share very similar toxicities. Collectively, these data suggest, that the entire structural configuration of AZAs is involved in the binding of the toxin to target proteins and bioassay data are required to characterize the impact of even minor structural differences.

In addition to the toxicological study, two quantitative methods, i.e., ELISA and LC-MS/MS (*m/z* 860>842 for AZA-59; *m/z* 842>824 for

Table 5
Relative cytotoxicity of various AZAs compared to AZA-1 (based on EC_{50} after 72 h incubation with Jurkat T lymphcytes).

Compound	rel. potency	Reference
AZA-2	8.30	Twiner et al., 2012b
AZA-3	4.50	
37-*epi*-AZA-1	5.10	Kilcoyne et al., 2014b
AZA-33	0.22	Kilcoyne et al., 2014c
AZA-34	5.50	
AZA-36	0.16	Krock et al., 2015
AZA-37	0.33	
AZA-26	0.03	Kilcoyne et al., 2018
AZA-59	**0.20**	this study

AZA-1) were compared. Both methods showed similar quantitative estimation of AZA-59 as quantified by qNMR and as AZA-1 equivalents. Therefore, external calibration of AZA-59 concentrations via the AZA-1 NRC standard will most likely serve as a good approximation until an analytical AZA-59 reference standard becomes available. However, this result is based on the quantitative results obtained for purified AZA standards dissolved in methanol on one LC-MS/MS instrument and should be thoroughly evaluated in a laboratory ring trial.

To date, AZA-59 in shellfish has only been found in samples from the Pacific Northwest coast of the US. The maximum detected concentration of 2.4 μg per kg (1.9 μg per kg in AZA-1 eq.) (Adams et al., 2020, unpublished data) thus far did not approach levels that would be a major cause for concern to food safety. However, *A. poporum* and AZA-59 are clearly present in the Puget Sound shellfish producing region and monitoring for *Azadinium* spp. is warranted, especially during algal bloom events. The potential biotransformation of AZA-59 in shellfish such as methyl or fatty acid esters should also be investigated.

In conclusion, the evaluation of the relative potency of AZA-59, the main AZA found in the Puget Sound region, yielded very similar toxic effects and lethal doses (TEF = 0.8) for AZA-59 in comparison to AZA-1. This data should serve as a good guideline to i) provide a regulatory threshold for AZA-59 in AZA-1 equivalents, as is the current practice in both the EU and the US, and ii) monitor for the presence of this toxin in shellfish, in the event that cell densities of *Azadinium* increase and/or AZA-59 concentrations in shellfish increase in the future, either in the US or other regions of the world where this toxin may occur.

Funding

This research was supported in part by (1) a grant from the NOAA NCCOS Monitoring and Event Response for Harmful Algal Blooms (MERHAB) research program, (2) a grant by the Helmholtz Association (PoF IV ST 6.1, 6.2), (3) by a contract to the University of Trieste by the United States Food and Drug Administration Center for Food Safety and Applied Nutrition, and (4) as part of the MARBioFEED project, supported under the First Call for Transnational Research Projects within the Marine Biotechnology ERA-NET; project no. 604,814. ("Enhanced Biorefining Methods for the Production of Marine Biotoxins and Microalgae Fish Feed"). This is MERHAB publication #249.

CRediT authorship contribution statement

Jan Tebben: Conceptualization, Visualization, Formal analysis, Writing – review & editing, Writing – original draft. **Christian Zurhelle:** Conceptualization, Visualization, Formal analysis, Writing – review & editing. **Aurelia Tubaro:** Formal analysis, Writing – review & editing. **Ingunn A. Samdal:** Formal analysis, Writing – review & editing. **Bernd Krock:** Formal analysis, Writing – review & editing. **Jane Kilcoyne:** Formal analysis, Writing – review & editing. **Silvio Sosa:** Conceptualization, Visualization, Formal analysis, Writing – review & editing, Writing – original draft. **Vera L. Trainer:** Conceptualization, Visualization, Formal analysis, Writing – review & editing, Project administration, Funding acquisition. **Jonathan R. Deeds:** Conceptualization, Visualization, Formal analysis, Writing – review & editing, Writing – original draft, Project administration, Funding acquisition. **Urban Tillmann:** Conceptualization, Visualization, Formal analysis, Writing – review & editing, Writing – original draft.

Declaration of Competing Interest

The authors declare that they have no known competing financial interests or personal relationships that could have appeared to influence the work reported in this paper.

Data availability

Data will be made available on request.

Acknowledgments

We thank the SoundToxins partnership for helping to identify *Azadinium* hotspots and Cheryl Greengrove (University of Washington), Brian Bill (NOAA) and Joo-Hwan Kim (Hanyang University) for providing and maintaining the sediment samples from Puget Sound needed to isolate the *Azadinium* strain used for toxin purification. We are grateful for suggestions in response to the Journal Pre-proof provided by Christopher Miles and Mitsunori Iwataki.

Supplementary materials

Supplementary material associated with this article can be found, in the online version, at doi:10.1016/j.hal.2023.102388.

References

Adams, N.G., Tillmann, U., Trainer, V.L., 2020. Temporal and spatial distribution of *Azadinium* species in the inland and coastal waters of the Pacific northwest in 2014-2018. Harmful Algae 98, 101874.

Alfonso, A., Roman, Y., Vieytes, M.R., Ofuji, K., Satake, M., Yasumoto, T., Botana, L.M., 2005. Azaspiracid-4 inhibits Ca2+ entry by stored operated channels in human T lymphocytes. Biochem. Pharmacol. 69 (11), 1627–1636.

Aune, T., Larsen, S., Aasen, J.A.B., Rehmann, N., Satake, M., Hess, P., 2007. Relative toxicity of dinophysistoxin-2 (DTX-2) compared with okadaic acid, based on acute intraperitoneal toxicity in mice. Toxicon 49 (1), 1–7.

Bellocci, M., Sala, G.L., Callegari, F., Rossini, G.P., 2010. Azaspiracid-1 inhibits endocytosis of plasma membrane proteins in epithelial cells. Toxicol. Sci. 117 (1), 109–121.

Boente-Juncal, A., Mendez, A.G., Vale, C., Vieytes, M.R., Botana, L.M., 2018. In vitro effects of chronic spirolide treatment on human neuronal stem cell differentiation and cholinergic system development. ACS Chem. Neurosci. 9 (6), 1441–1452.

Boente-Juncal, A., Raposo-Garcia, S., Costas, C., Louzao, M.C., Vale, C., Botana, L.M., 2020. Partial blockade of human voltage-dependent sodium channels by the marine toxins azaspiracids. Chem. Res. Toxicol. 33 (10), 2593–2604.

Boente-Juncal, A., Raposo-Garcia, S., Louzao, M.C., Vale, C., Botana, L.M., 2021. Targeting chloride ion channels: new insights into the mechanism of action of the marine toxin azaspiracid. Chem. Res. Toxicol.

Dai, X., Bill, B.D., Adams, N.G., Tillmann, U., Sloan, C., Lu, D., Trainer, V.L., 2019. The effect of temperature and salinity on growth rate and azaspiracid concentration in two strains of *Azadinium poporum* (Dinophyceae) from Puget Sound, Washington State. Harmful Algae 89, 101665.

EFSA (European Food Safety Authority), 2008. Marine biotoxins in shellfish – azaspiracid group - scientific opinion of the panel on contaminants in the food chain. EFSA J. 6 (10), 723.

FDA (United States Food and Drug Administration), 2022. Fish and Fishery Products Hazards and Controls Guidance, 2022. Edition, Appendix 5: FDA and EPA Safety Levels in Regulations and Guidance. US Food and Drug Administration, Washington D.C. Available at: https://www.fda.gov/food/seafood-guidance-documents-regulatory-information/fish-and-fishery-products-hazards-and-controls (accessed 30 November 2022).

Ferreiro, S.F., Vilarino, N., Louzao, M.C., Nicolaou, K.C., Frederick, M.O., Botana, L.M., 2014. In vitro chronic effects on hERG channel caused by the marine biotoxin azaspiracid-2. Toxicon 91, 69–75.

Finney, D.J., 1971. Probit Analysis, 3rd edition. Cambridge University Press, Cambridge.

Furey, A., O'Doherty, S., O'Callaghan, K., Lehane, M., James, K.J., 2010. Azaspiracid poisoning (AZP) toxins in shellfish: toxicological and health considerations. Toxicon 56 (2), 173–190.
Furrer, J., 2010. A robust, sensitive, and versatile HMBC experiment for rapid structure elucidation by NMR: IMPACT-HMBC. Chem. Commun. 46 (19), 3396–3398.
Hess, P., Twiner, M.J., Kilcoyne, J., Sosa, S., 2014. Azaspiracid toxins: toxicological profile. In: Gopalakrishnakone, P., Haddad Jr., V., Kem, W.R., Tubaro, A., Kim, E. (Eds.), Marine and Freshwater Toxins. Springer Netherlands, Dordrecht, pp. 1–19.
Ito, E., Frederick, M.O., Koftis, T.V., Tang, W.J., Petrovic, G., Ling, T.T., Nicolaou, K.C., 2006. Structure toxicity relationships of synthetic azaspiracid-1 and analogs in mice. Harmful Algae 5 (5), 586–591.
Ito, E., Satake, M., Ofuji, K., Higashi, M., Harigaya, K., McMahon, T., Yasumoto, T., 2002. Chronic effects in mice caused by oral administration of sublethal doses of azaspiracid, a new marine toxin isolated from mussels. Toxicon 40 (2), 193–203.
Ito, E., Satake, M., Ofuji, K., Kurita, N., McMahon, T., James, K., Yasumoto, T., 2000. Multiple organ damage caused by a new toxin azaspiracid, isolated from mussels produced in Ireland. Toxicon 38 (7), 917–930.
Ito, E., Terao, K., MacMahon, T., Silke, J., Yasumoto, T., 1998. Acute pathologicl changes in mice caused by crude extracts of novel toxins isolated from Irish mussels. In: Reguera, B., Blanco, J., Fernandez, M.L., Wyatt, T. (Eds.), Harmful Algae. Xunta de Galicia and Intergovernmental Oceanographic Commission of UNESCO, Vigo, pp. 588–589.
Keller, M.D., Selvin, R.C., Claus, W., Guillard, R.R.L., 1987. Media for the culture of oceanic ultraphytoplankton. J. Phycol. 23 (4), 633–638.
Kellmann, R., Schaffner, C.A.M., Gronset, T.A., Satake, M., Ziegler, M., Fladmark, K.E., 2009. Proteomic response of human neuroblastoma cells to azaspiracid-1. J. Proteomics 72 (4), 695–707.
Kenton, N.T., Adu-Ampratwum, D., Okumu, A.A., McCarron, P., Kilcoyne, J., Rise, F., Wilkins, A.L., Miles, C.O., Forsyth, C.J., 2018a. Stereochemical Definition of the Natural Product (6R,10R,13R,14R,16R,17R,19S,20S,21R,24S,25S,28S,30S,32R,33R,34R,36S,37S, 39R)-Azaspiracid-3 by Total Synthesis and Comparative Analyses. Angewandte Chemie-International Edition 57 (3), 810–813.
Kenton, N.T., Adu-Ampratwum, D., Okumu, A.A., Zhang, Z.G., Chen, Y., Nguyen, S., Xu, J.Y., Ding, Y., McCarron, P., Kilcoyne, J., Rise, F., Wilkins, A.L., Miles, C.O., Forsyth, C.J., 2018b. Total Synthesis of (R,10R,13R,14R,16R,17R,19S,20R,21R,24S,25S,28S,30S,32R,33R,34R,36S,37S, 39R)-Azaspiracid-3 Reveals Non-Identity with the Natural Product. Angewandte Chemie-International Edition 57 (3), 805–809.
Kilcoyne, J., Jauffrais, T., Twiner, M.J., Doucette, G.J., Aasen Bunes, J.A., Sosa, S., Krock, B., Séhet, V., Nulty, C., Salas, R., Clarke, D., Geraghty, J., Duffy, C., Foley, B., John, U., Quilliam, M.A., McCarron, P., Miles, C.O., Silke, J., Cembella, A., Tillmann, U., Hess, P., 2014a. AZASPIRACIDS – toxicological evaluation, test methods and identifcation of the source organisms (ASTOX II). Technical Report Marine Institutem Galway 188. Ireland (2014) (ISSN:2009-3195.
Kilcoyne, J., McCarron, P., Twiner, M.J., Nulty, C., Crain, S., Quilliam, M.A., Rise, F., Wilkins, A.L., Miles, C.O., 2014b. Epimers of azaspiracids: isolation, structural elucidation, relative LC-MS response, and in vitro toxicity of 37-*epi*-azaspiracid-1. Chem. Res. Toxicol. 27 (4), 587–600.
Kilcoyne, J., McCarron, P., Twiner, M.J., Rise, F., Hess, P., Wilkins, A.L., Miles, C.O., 2018. Identification of 21,22-dehydroazaspiracids in mussels (*Mytilus edulis*) and in vitro toxicity of azaspiracid-26. J. Nat. Prod. 81 (4), 885–893.
Kilcoyne, J., Nulty, C., Jauffrais, T., McCarron, P., Herve, F., Foley, B., Rise, F., Crain, S., Wilkins, A.L., Twiner, M.J., Hess, P., Miles, C.O., 2014c. Isolation, Structure Elucidation, Relative LC-MS Response, and *in Vitro* Toxicity of azaspiracids from the Dinoflagellate *Azadinium spinosum*. J. Nat. Prod. 77 (11), 2465–2474.
Kilcoyne, J., Keogh, A., Clancy, G., LeBlanc, P., Burton, I., Quilliam, M.A., Hess, P., Miles, C.O., 2012. Improved isolation procedure for azaspiracids from shellfish, structural elucidation of azaspiracid-6, and stability studies. J. Agric. Food Chem. 60 (10), 2447–2455.
Kim, J.H., Tillmann, U., Adams, N.G., Krock, B., Stutts, W.L., Deeds, J.R., Han, M.S., Trainer, V.L., 2017. Identification of *Azadinium* species and a new azaspiracid from *Azadinium poporum* in Puget Sound, Washington State, USA. Harmful Algae 68, 152–167.
Krock, B., Tillmann, U., Potvin, E., Jeong, H.J., Drebing, W., Kilcoyne, J., Al-Jorani, A., Twiner, M.J., Gothel, Q., Köck, M., 2015. Structure elucidation and in vitro toxicity of new azaspiracids isolated from the marine dinoflagellate *Azadinium poporum*. Mar. Drugs 13 (11), 6687–6702.
Krock, B., Tillmann, U., Tebben, J., Trefault, N., Gu, H.F., 2019. Two novel azaspiracids from *Azadinium poporum*, and a comprehensive compilation of azaspiracids produced by Amphidomataceae, (Dinophyceae). Harmful Algae 82, 1–8.
Kulagina, N.V., Twiner, M.J., Hess, P., McMahon, T., Satake, M., Yasumoto, T., Ramsdell, J.S., Doucette, G.J., Ma, W., O'Shaughnessy, T.J., 2006. Azaspiracid-1 inhibits bioelectrical activity of spinal cord neuronal networks. Toxicon 47 (7), 766–773.
Luo, Z., Krock, B., Giannakourou, A., Venetsanopoulou, A., Pagou, K., Tillmann, U., Gu, H., 2018. Sympatric occurrence of two *Azadinium poporum* ribotypes in the Eastern Mediterranean Sea. Harmful Algae 78, 75–85.
Nicolaou, K.C., Chen, D.Y.K., Li, Y.W., Qian, W.Y., Ling, T.T., Vyskocil, S., Koftis, T.V., Govindasamy, M., Uesaka, N., 2003a. Total synthesis of the proposed azaspiracid-1 structure, part 2: Coupling of the C1-C20, C21-C27, and C28-C40 fragments and completion and synthesis. Angewandte Chemie-International Edition 42 (31), 3649–3653.
Nicolaou, K.C., Li, Y.W., Uesaka, N., Koftis, T.V., Vyskocil, S., Ling, T.T., Govindasamy, M., Qian, W., Bernal, F., Chen, D.Y.K., 2003b. Total synthesis of the proposed azaspiracid-1 structure, part 1: Construction of the enantiomerically pure C1-C20, C21-C27, and C28-C40 fragments. Angewandte Chemie-International Edition 42 (31), 3643–3648.
Nicolaou, K.C., Koftis, T.V., Vyskocil, S., Petrovic, G., Ling, T.T., Yamada, Y.M.A., Tang, W.J., Frederick, M.O., 2004a. Structural revision and total synthesis of azaspiracid-1, part 2: Definition of the ABCD domain and total synthesis. Angewandte Chemie-International Edition 43 (33), 4318–4324.
Nicolaou, K.C., Vyskocil, S., Koftis, T.V., Yamada, Y.M.A., Ling, T.T., Chen, D.Y.K., Tang, W.J., Petrovic, G., Frederick, M.O., Li, Y.W., Satake, M., 2004b. Structural revision and total synthesis of azaspiracid-1, part 1: Intelligence gathering and tentative proposal. Angewandte Chemie-International Edition 43 (33), 4312–4318.
Ofuji, K., Satake, M., McMahon, T., Silke, J., James, K.J., Naoki, H., Oshima, Y., Yasumoto, T., 1999. Two analogs of azaspiracid isolated from mussels, *Mytilus edulis*, involved in human intoxication in Ireland. Nat. Toxins 7 (3), 99–102.
Pelin, M., Kilcoyne, J., Florio, C., Hess, P., Tubaro, A., Sosa, S., 2019. Azaspiracids increase mitochondrial dehydrogenases activity in hepatocytes: involvement of potassium and chloride ions. Mar Drugs 17 (5).
Pelin, M., Kilcoyne, J., Nulty, C., Crain, S., Hess, P., Tubaro, A., Sosa, S., 2018. Toxic equivalency factors (TEFs) after acute oral exposure of azaspiracid 1,-2 and-3 in mice. Toxicol. Lett. 282, 136–146.
Roman, Y., Alfonso, A., Louzao, M.C., de la Rosa, L.A., Leira, F., Vieites, J.M., Vieytes, M. R., Ofuji, K., Satake, M., Yasumoto, T., Botana, L.M., 2002. Azaspiracid-1, a potent, nonapoptotic new phycotoxin with several cell targets. Cell. Signal. 14 (8), 703–716.
Ronzitti, G., Hess, P., Rehmann, N., Rossini, G.P., 2007. Azaspiracid-1 alters the E-cadherin pool in epithelial cells. Toxicol. Sci. 95 (2), 427–435.
Samdal, I.A., Lovberg, K.E., Briggs, L.R., Kilcoyne, J., Xu, J.Y., Forsyth, C.J., Miles, C.O., 2015. Development of an ELISA for the detection of Azaspiracids. J. Agric. Food Chem. 63 (35), 7855–7861.
Samdal, I.A., Lovberg, K.E., Kristoffersen, A.B., Briggs, L.R., Kilcoyne, J., Forsyth, C.J., Miles, C.O., 2019. A Practical ELISA for Azaspiracids in Shellfish via Development of a New Plate-Coating Antigen. J. Agric. Food Chem. 67 (8), 2369–2376.
Sandvik, M., Miles, C.O., Løvberg, K.L.E., Kryuchkov, F., Wright, E.J., Mudge, E.M., Kilcoyne, J., Samdal, I.A., 2021. In Vitro Metabolism of Azaspiracids 1–3 with a Hepatopancreatic Fraction from Blue Mussels (*Mytilus edulis*). Journal of Agricultural and Food Chemistry 69 (38), 11322–11335.
Satake, M., Ofuji, K., James, K., Furey, A., Yasumoto, T., 1998a. New toxic event caused by Irish mussels. In: Reguera, B., Blanco, J., Fernandez, M.L., Wyatt, T. (Eds.), Intergovernmental Oceanographic Commission of UNESCO. Paris, France, pp. 68–469.
Satake, M., Ofuji, K., Naoki, H., James, K.J., Furey, A., McMahon, T., Silke, J., Yasumoto, T., 1998b. Azaspiracid, a new marine toxin having unique spiro ring assemblies, isolated from Irish mussels, *mytilus edulis*. J. Am. Chem. Soc. 120 (38), 9967–9968.
Tillmann, U., 2018. Amphidomataceae. In: Shumway, S.E., Burkholder, J.M., Morton, S. L. (Eds.), Harmful Algal blooms: a Compendium Desk Reference. John Wiley & Sons, Hoboken, pp. 575–582.
Tillmann, U., Elbrächter, M., Krock, B., John, U., Cembella, A., 2009. *Azadinium spinosum* gen. et sp. nov. (Dinophyceae) identified as a primary producer of azaspiracid toxins. Eur. J. Phycol. 44 (1), 63–79.
Trainer, V.L., Moore, L., Bill, B.D., Adams, N.G., Harrington, N., Borchert, J., da Silva, D. A., Eberhart, B.T., 2013. Diarrhetic shellfish toxins and other lipophilic toxins of human health concern in Washington State. Mar Drugs 11 (6), 1815–1835.
Twiner, M.J., Doucette, G.J., Rasky, A., Huang, X.P., Roth, B.L., Sanguinetti, M.C., 2012a. Marine algal toxin azaspiracid is an open-state blocker of hERG potassium channels. Chem. Res. Toxicol. 25 (9), 1975–1984.
Twiner, M.J., El-Ladki, R., Kilcoyne, J., Doucette, G.J., 2012b. Comparative effects of the marine algal toxins azaspiracid-1,-2, and-3 on Jurkat T lymphocyte cells. Chem. Res. Toxicol. 25 (3), 747–754.
Twiner, M.J., Hanagriff, J.C., Butler, S., Madhkoor, A.K., Doucette, G.J., 2012c. Induction of apoptosis pathways in several cell lines following exposure to the marine algal toxin azaspiracid. Chem. Res. Toxicol. 25 (7), 1493–1501.
Twiner, M.J., Hess, P., Dechraoui, M.Y.B., McMahon, T., Samons, M.S., Satake, M., Yasumoto, T., Ramsdell, J.S., Doucette, G.J., 2005. Cytotoxic and cytoskeletal effects of azaspiracid-1 on mammalian cell lines. Toxicon 45 (7), 891–900.
Twiner, M.J., Rehmann, N., Hess, P., Doucette, G.J., 2008. Azaspiracid shellfish poisoning: a review on the chemistry, ecology, and toxicology with an emphasis on human health impacts. Mar. Drugs 6 (2), 39–72.
Vale, C., Gomez-Limia, B., Nicolaou, K.C., Frederick, M.O., Vieytes, M.R., Botana, L.M., 2007a. The c-Jun-N-terminal kinase is involved in the neurotoxic effect of azaspiracid-1. Cellular Physiol. Biochem. 20 (6), 957–966.
Vale, C., Nicolaou, K.C., Frederick, M.O., Gomez-Limia, B., Alfonso, A., Vieytes, M.R., Botana, L.M., 2007b. Effects of azaspiracid-1, a potent cytotoxic agent, on primary neuronal cultures. A structure-activity relationship study. J. Med. Chem. 50 (2), 356–363.
Vale, C., Wandscheer, C., Nicolaou, K.C., Frederick, M.O., Alfonso, C., Vieytes, M.R., Botana, L.M., 2008. Cytotoxic effect of azaspiracid-2 and azaspiracid-2-methyl ester in cultured neurons: involvement of the c-Jun N-terminal kinase. J. Neurosci. Res. 86 (13), 2952–2962.
Vilarino, N., Nicolaou, K.C., Frederick, M.O., Cagide, E., Alfonso, C., Alonso, E., Vieytes, M.R., Botana, L.M., 2008. Azaspiracid substituent at C1 is relevant to in vitro toxicity. Chem. Res. Toxicol. 21 (9), 1823–1831.
Vilarino, N., Nicolaou, K.C., Frederick, M.O., Vieytes, M.R., Botana, L.M., 2007. Irreversible cytoskeletal disarrangement is independent of caspase activation during in vitro azaspiracid toxicity in human neuroblastoma cells. Biochem. Pharmacol. 74 (2), 327–335.